LM-04K048
June 9, 2004

High Performance InGaAsSb TPV Cells

ZA Shellengarger, GC Taylor, RU Martinelli and JM Carpinelli

NOTICE

This report was prepared as an account of work sponsored by the United States Government. Neither the United States, nor the United States Department of Energy, nor any of their employees, nor any of their contractors, subcontractors, or their employees, makes any warranty, express or implied, or assumes any legal liability or responsibility for the accuracy, completeness or usefulness of any information, apparatus, product or process disclosed, or represents that its use would not infringe privately owned rights.

High Performance InGaAsSb TPV Cells

Zane A. Shellenbarger, Gordon C. Taylor, Ramon U. Martinelli, and Joseph M. Carpinelli

Sarnoff Corporation
Princeton, New Jersey 08543

Abstract. Lattice-matched 0.52 eV InGaAsSb/GaSb thermophotovoltaic (TPV) cells are grown using a multi-wafer metal-organic-chemical-vapor-deposition (MOCVD) system. MOCVD growth series of P/N junction epitaxial structures consisting of as many as 30 wafers demonstrate good run-to-run reproducibility, good uniformity across the wafer and exhibit high performance with open circuit voltages of ~300mV and fill factors of 70% at 25°C. Growth parameters, including temperature, surface preparation and substrate orientation, that directly affect growth have been optimized for the active 0.52 eV InGaAsSb region and GaSb confinement layers. Focus is on increasing TPV diode performance through architectural improvements, specifically by reducing the minority carrier recombination velocity at the emitter and base front and back interfaces. Work in support of incorporating a back surface reflector (BSR) including the growth of N/P diode architectures and the addition of a lattice-matched InAsSb etch stop layer for substrate removal and wafer bonding, is reported. The lattice matched InAsSb stop etch exhibits resiliency to the substrate removal and wafer bonding processes. Substantial improvement in carrier lifetime on test structures with P-type AlGaAsSb layers indicated incorporation of these layers into the TPV cell structure should provide significant improvement in open-circuit voltage. Addition of AlGaAsSb confinement layers to the standard P/N cell structure gave some of the best InGaAsSb TPV cell results to date.

INTRODUCTION

Continued development of thermophotovoltaic (TPV) systems to exploit available thermal sources offers the potential for high conversion efficiency systems in a variety of applications. To achieve high efficiencies with many available sources, devices in low bandgap semiconductors are required. One low bandgap material system, the quaternary InGaAsSb, has the advantage of being lattice matched to available GaSb wafers, thus offering the possibility of a low concentration of crystalline defects with consequently good carrier lifetimes [1, 2]. Sarnoff uses MOCVD to prepare TPV cells in this material. Modules incorporating these TPV cells have demonstrated greater than 19% power conversion efficiency from a 950 °C blackbody source [3]. In this paper, we report the current state-of-the-art in preparation of standard P/N architecture InGaAsSb TPV cells as well as current work on improving diode performance through reduced carrier recombination at the interfaces and incorporation of a back surface reflector. Special structures grown to facilitate measurement of minority carrier lifetime are also presented.

STANDARD P/N ARCHITECTURE CELLS

The active material, InGaAsSb, of the P/N cells is prepared by MOCVD on GaSb substrates. The target composition is $In_{0.16}Ga_{0.84}As_{0.14}Sb_{0.86}$ with a 0.53 eV bandgap. A low-pressure, vertical rotating-disk reactor with capacity for three two-inch wafers is used. The system has a vertical gas flow, high-speed rotation, and a turbo-pumped low-pressure load-lock. Precursors used are triethylgallium (TEG), trimethylindium (TMI), trimethylantimony (TMSb), and 1000-ppm arsine (AsH_3) in hydrogen. The dopants used are 1000 ppm dimethylzinc (DMZ) in hydrogen for P-type material and 100 ppm diethyltelluride (DETe) in hydrogen for N-type material. Typical growth conditions are 60 torr pressure, 100 rpm wafer rotation, and 19 slpm H_2 carrier gas flow. Achievement of high material quality for this low bandgap composition depends strongly on temperature and substrate orientation. The typical growth temperature is 525°C and best results were achieved using (100) substrates misoriented 6° towards the (111)B direction. The structure of the cells is schematically illustrated in Figure 1.

Layer	Thickness
p^+ – GaSb	0.1-0.5 μm
p – 0.53 eV InGaAsSb	5-7 μm
n – 0.53eV InGaAsSb	1-3 μm
n – GaSb	0.2-0.5 μm
Te-doped GaSb substrate n – $5x10^{17}cm^{-3}$	

FIGURE 1. Schematic device layer structure.

Material uniformity is essential for a good yield of high efficiency cells. Properties of the layers are assessed with double-crystal X-ray diffraction, photoluminescence (PL), and Hall measurements. Photoluminescence, which is the key measure of uniformity, is recorded at the center of the wafer and at four points 5 mm from the edge of the wafer. For three wafers from a single growth run, variation in the peak PL from the center of the wafers is typically within ± 3 nm. Variation in the peak PL from the center of the wafers from run to run is typically within ± 6 nm.

Data indicate almost identical properties for the three wafers from a single growth run. To demonstrate reproducibility, a production growth series of 30 wafers was done. For the 30 wafers, the average peak PL at the center of the wafer was 2351 nm with a standard deviation of 9 nm and the average lattice mismatch was 0.074% with a standard deviation of 0.03%. These observations suggest that material can be prepared in reasonable volume for the fabrication of TPV cells.

Fabrication of the P/N cells begins with steps to remove contaminants and surface oxides. The N-type contact metal consists of Au/Ti/Pt/Au (50nm/30nm/100nm/200nm). The ohmic contact is formed by RTA sintering in forming gas at 300 °C for 60 seconds. The Ti/Pt layer prevents interaction of the top

gold layer with the GaSb during the sintering process, preserving a good surface for solder mounting the completed device at the end of the process.

A relatively simple two layer photoresist process is used to pattern the P-contact metal by the lift-off process. The first layer of positive photoresist, nominally 4 μm thick, is spun on and baked at 85 °C. Next, a 120 nm film of aluminum is deposited in a thermal evaporation system. A second photoresist layer is then applied and baked at 65 °C. The grid pattern is exposed and developed in the top photoresist layer. The pattern is then transferred into the aluminum layer by etching in concentrated phosphoric acid. Next the wafer is uniformly exposed without a photomask and developed. This patterns the bottom photoresist layer and slightly undercuts the aluminum layer, to facilitate the lift-off of a thick metal layer. After removing surface oxides in a 1:10 dilution of ammonium hydroxide in de-ionized water for 60 seconds, the wafer is metallized. The P-contact metal consists of Ti/Pt/Ag/Pt/Au (30nm/100nm/5000nm/100nm/200nm). After deposition, the unwanted metal is removed by soaking in acetone to dissolve the photoresist and wash away the metal lying on top of it. No additional heat treatment is required to form ohmic contacts to the P-type layer. Specific contact resistances measured by the Cox and Strack method showed 2.5×10^{-5} Ω-cm^2 for the sintered N-contacts and 6.0×10^{-6} Ω-cm^2 for the P-contacts.

Finally, the wafer is protected by a thin layer of positive photoresist, and cleaved into individual cells. Any mechanical damage at the cell edges is removed by chemically etching in a 10:1 mixture of 50W% citric acid and hydrogen peroxide. Removal of approximately 1 μm from the cell edges is adequate to obtain cells with high shunt resistance.

Each wafer is processed into 24 standard cells with dimensions 5 mm × 10 mm as well as 4 mm × 4 mm test cells and other test structures as shown in Figure 2. Although the layouts for the current collection grids are slightly different, basically the grids of the two cells consist of 10 μm wide lines on a 100 μm spacing with one bus bar. The data indicate that good uniformity and yield from multiple wafers are achievable.

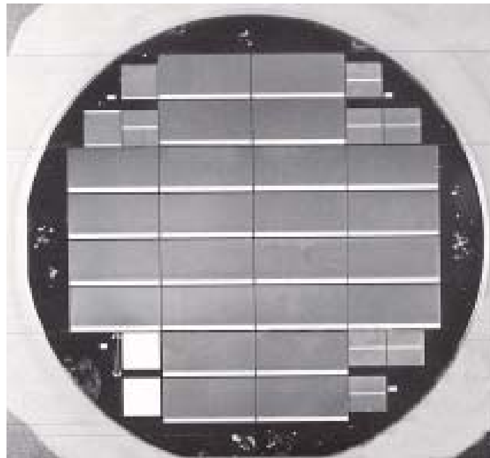

FIGURE 2. Fabricated TPV cell wafer.

A variety of measurements are done to evaluate the TPV cells. Dark current-voltage characteristics are used to extract the zero-bias slope as the shunt resistance. This definition of shunt resistance yields a good fit to a model calculation. Short circuit current versus open circuit voltage plots for different light intensities yield the diode ideality factor, n, and the dark current density, J_0. Output characteristics with illumination to a short circuit current density of 2 A/cm^2 are used to determine fill factor and open circuit voltage. Finally, spectral quantum efficiency (SQE) of the cells is determined from an absolute measurement at 1.55 μm and from the relative SQE in the range from 1.0 to 2.6 μm.

For most of the measurements discussed here, the cells were packaged by soldering them onto a brass pallet with a lead attached along the main bus bar to minimize external series resistance. The pallet serves as a heat sink and is attached to a water-cooled copper block for measurements. Open circuit voltage measurements indicate that there is no appreciable temperature rise during the measurements.

Statistical data for the device results on fabricated TPV cells indicate that good uniformity and yield for devices from multiple wafers is achievable. Standard deviations less than 3% for maximum QE, open circuit voltage, and fill factor over whole wafers were demonstrated. The results from current-voltage measurements on a typical wafer conducted by a robotic measurement system at Lockheed Martin using a flash lamp are shown in Figure 3. These results were repeatable from run to run.

Voc (mV)			
	277	281	
	273	275	
283	274	282	278
278	275	278	280
279	277	281	279
283	280	276	285
	278	283	
	281	281	

average 279.0 mV
std. dev. 3.1

Isc (mA)			
	950	947	
	898	946	
934	936	975	963
898	903	973	958
918	923	928	967
920	947	885	955
	945	934	
	957	964	

average 938.5 mA
std. dev. 25.1

FF (%)			
	68	69	
	66	61	
67	62	61	66
68	70	68	68
68	70	69	69
71	70	68	71
	69	67	
	70	70	

average 67.8 %
std. dev. 2.8

FIGURE 3. Current-voltage measurement results across wafer.

REDUCTION OF INTERFACE RECOMBINATION

A substantial improvement in V_{oc} should be obtained from reduction of recombination at the InGaAsSb/GaSb interface. Using a larger bandgap material such as AlGaAsSb for confinement layers should reduce this recombination. Growth conditions for optimum X-ray and surface morphology of AlGaAsSb with Al content up to 50% were determined. Growth temperature is the same as InGaAsSb (525°C).

Undoped and Zn-doped material with 30% Al has excellent surface morphology and lattice matching. The background P-doping of undoped material is 3-4 × 10^{17} cm^{-3}. Using Te doping, N-type concentrations up to 2 × 10^{17} cm^{-3} with good material quality were obtained.

Double heterostructure P-type lifetime structures were grown with AlGaAsSb confinement layers. PL intensity was higher than standard material with a GaSb cap layer. Photoluminescence decay lifetimes as high as 350 ns were measured at SUNY at Stony Brook. Assuming the lifetime is limited by the interfacial recombination velocity, this implies a maximum value of interfacial recombination velocity of 72 cm/s. Additional N-type lifetime samples were grown as well. Lifetimes were approximately a factor of three shorter than equivalently doped P-type structures. Further analysis of N-type material is ongoing.

TPV cell wafers incorporating AlGaAsSb confinement layers were grown and processed. These cells had similar P/N structure to the cells shown in Figure 1 but with the addition of a 30 nm thick AlGaAsSb layer above and below the InGaAsSb layers. These cells showed improved device characteristics and also demonstrated some dependence of the cell results on bandgap of the InGaAsSb material.

A correlation between the bandgap, E_g, of the emitter of a TPV cell and the cell's V_{oc}, I_{sc}, and J_0 has been made on cells from a set of four wafers grown with the AlGaAsSb confinement layers. Cells measured at Sarnoff were standard 4 × 4 mm^2 test structures. The bandgap was obtained from the cells' spectral quantum efficiency characteristic and is defined as the 50% point of the quantum efficiency in the long-wavelength-cut-off region as shown in Figure 4. Figure 5 shows V_{oc} and J_0 as functions of E_g.

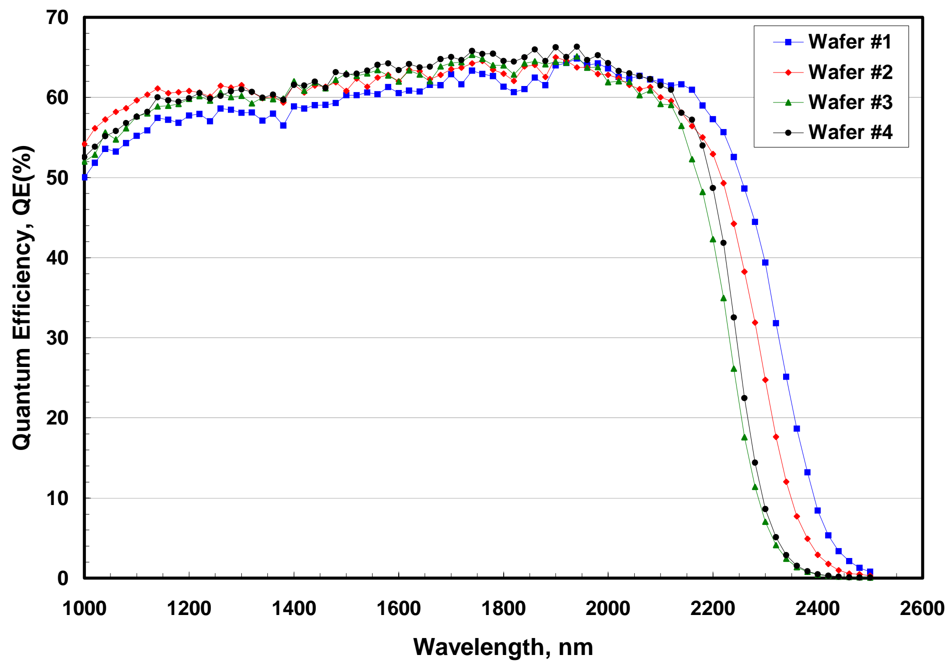

FIGURE 4. External spectral quantum efficiency characteristics.

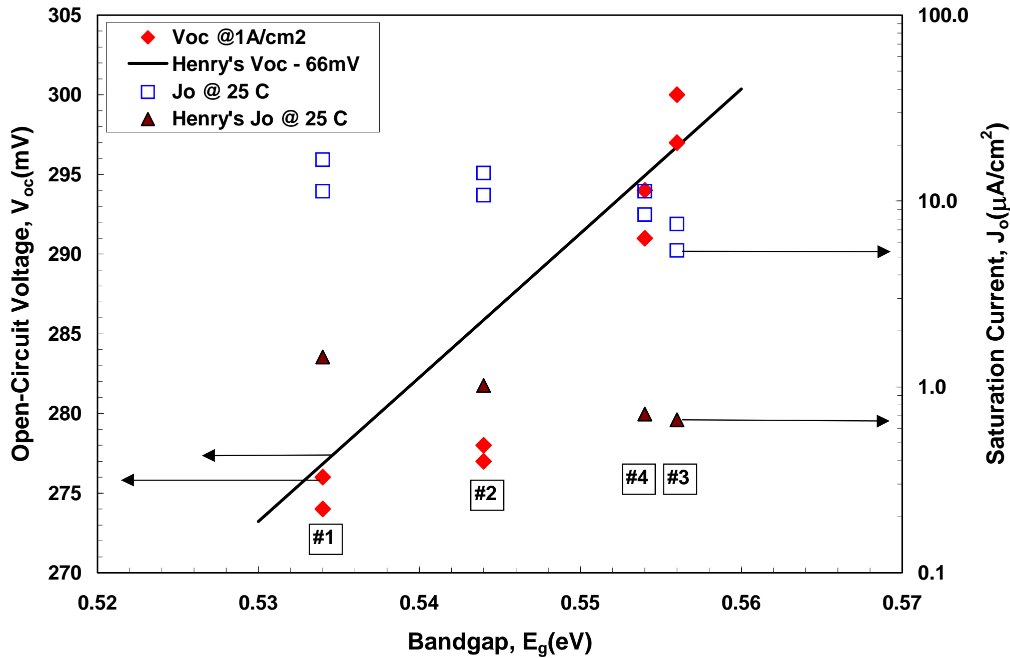

FIGURE 5. Dependence of V_{oc} (diamonds) and J_0 (squares) on bandgap for TPV cells from four different wafers having slightly different bandgap (2 cells from each wafer). Also shown is Henry's calculation of J_0 (triangles) and V_{oc} (solid line), adjusted to equal the highest V_{oc}.

As E_g increases, V_{oc} increases and J_0 decreases, as expected qualitatively. A plot of C. H. Henry's calculation of thermodynamically limited $V_{oc}(E_g)$ [4] has the same slope as the measured V_{oc} data; the calculated curve is adjusted to agree with the V_{oc} data at $E_g = 0.56$ eV by subtracting 66 mV. This subtraction accounts for the cells' saturation current being larger than the thermodynamic limit, which leads to a smaller V_{oc}. The 66 mV shift implies a dark current density that is about a factor of 10 larger than Henry's thermodynamic lower limit which is what we observe. It appears that the increase in V_{oc} in these samples is determined by the increase in the bandgap.

These results imply that the larger values of V_{oc} measured for cells from wafers #3 and #4 arise, in part, from the larger InGaAsSb bandgaps in these cells. Minority-carrier lifetime also influences V_{oc}. Larger bandgap material may also have a longer minority-carrier lifetime, since the composition is farther from the InGaAsSb miscibility gap.

ADDITION OF BACK SURFACE REFLECTOR

More effective spectral utilization can be achieved in the InGaAsSb TPV cells if longer wavelength radiation and recycled photons are reflected at the back surface of the cell. Unfortunately, the conducting GaSb substrate has high free carrier absorption which makes this ineffective for full thickness wafers. Two methods to alleviate this problem are to remove most of the GaSb substrate (hybrid technique) or all of the substrate (wafer transfer technique). These techniques also make fabrication of a monolithically interconnected module (MIM) structure feasible, where smaller area

TPV cell segments are connected in series on the wafer. Growth development to support these techniques was developed at Sarnoff. The wafer structure required is shown in Figure 8.

Layer
N+ GaSb 0.2-0.7 μm
N InGaAsSb 0.2-1.0 μm
P InGaAsSb 4.0-6.0 μm
P GaSb 0.2-0.7μm
InAsSb etch stop 0.5-1.5 μm
P GaSb substrate

FIGURE 8. Growth structures to support back surface reflector incorporation.

The N/P architecture is preferred for both the "hybrid" and "wafer transfer" techniques since no sintering of the P-type metallization is required after the wafer has been epoxied down. The wafer transfer technique additionally requires a chemical etch-stop layer. Chemistry has been developed which allows lattice matched InAsSb to be used for this purpose.

Initial N/P cells without the InAsSb etch-stop were grown and processed. Electrical results were very promising with V_{oc} of 314 mV at I_{sc} of 0.818 A which is similar to the very best P/N structure cells. FF was very high at 71%.

Growth of new material, InAsSb lattice matched to GaSb was calibrated. Growth conditions for optimum X-ray and surface morphology were determined at the same growth temperature as InGaAsSb (525°C). A major growth difference from other antimonide compounds is the use of ~10X increase in V/III ratio to ~35. Under these conditions surface is mirror like with very few defects. Several wafers were grown with single 1 μm thick layers of InAsSb. These were used for etch-stop experiments where the substrate was completely removed leaving the InAsSb. The layers were smooth and continuous after substrate removal.

The complete N/P structure cell on InAsSb etch-stop layer was grown. Surface morphology and X-ray measurements indicate no major differences in the InGaAsSb material quality compared to growth without the etch-stop layer. The processing and testing of this material is currently under development.

SUMMARY

InGaAsSb TPV cells with layers grown by MOCVD in a multi-wafer reactor are produced with fill factors near 70% and with a peak external quantum efficiency

greater than 60%. Growth series with as many as 30 wafers show good control and uniformity of material composition and TPV cell electrical characteristics. Improvement to the standard P/N structure cell was made by addition of AlGaAsSb confinement layers to reduce interface recombination. New growth structures were developed to support incorporation of a back surface reflector into the InGaAsSb TPV cell.

ACKNOWLEDGEMENTS

This work was supported by Lockheed Martin. Special thanks go to Lee Danielson at Lockheed Martin for device measurements, Dmitri Donetski at SUNY at Stony Brook for carrier lifetime measurements and Dan Taylor at Bandwidth Semiconductor for processing of N/P material and back surface reflector structures.

REFERENCES

1. C. A. Wang, H. K. Choi, G. W. Turner, D. L. Spears, and M. J. Manfra, "Lattice-Matched Epitaxial GaInAsSb/GaSb Thermophotovoltaic Devices," in Thermophotovoltaic Generation of Electricity, Third Conference, edited by T. J. Coutts et al., *AIP Conference Proceedings* **401**, 75-87 (1997).
2. G. W. Charache, P. F. Baldasaro, L. R. Danielson, D. M. DePoy, M. J. Freeman, C. A. Wang, H. K. Choi, D. Z. Garbuzov, R. U. Martinelli, V. Khalfin, S. Saroop, J. M. Borrego, and R. J. Gutmann, "InGaAsSb thermophotovoltaic diode: Physics evaluation," *J. Appl. Phys*., **85**, 2247-2252 (1999).
3. Y. Z. Yu, R. U. Martinelli, G. C. Taylor, Z. Shellenbarger, R. K. Smeltzer, K. Palit, and D. Channin, "High-Efficiency Multi-Cell TPV Module Fabrication and Performance," in Thermophotovoltaic Generation of Electricity, Fifth Conference, edited by T. J. Coutts et al., *AIP Conference Proceedings* **653**, 335-343 (2002).
4. C. H. Henry, *J. Appl. Phys*., **51**, 4497 (1980).